

# Multi-modal Entity Alignment in Hyperbolic Space

Hao Guo, Jiuyang Tang, Weixin Zeng, Xiang Zhao, Li Liu

*National University of Defense Technology, China*

---

## Abstract

Many AI-related tasks involve the interactions of data in multiple modalities. It has been a new trend to merge multi-modal information into knowledge graph(KG), resulting in multi-modal knowledge graphs (MMKG). However, MMKGs usually suffer from low coverage and incompleteness. To mitigate this problem, a viable approach is to integrate complementary knowledge from other MMKGs. To this end, although existing entity alignment approaches could be adopted, they operate in the Euclidean space, and the resulting Euclidean entity representations can lead to large distortion of KG’s hierarchical structure. Besides, the visual information has yet not been well exploited.

In response to these issues, in this work, we propose a novel multi-modal entity alignment approach, Hyperbolic multi-modal entity alignment (HMEA), which extends the Euclidean representation to hyperboloid manifold. We first adopt the Hyperbolic Graph Convolutional Networks (HGCNs) to learn structural representations of entities. Regarding the visual information, we generate image embeddings using the `densenet` model, which are also projected into the hyperbolic space using HGCNs. Finally, we combine the structure and visual representations in the hyperbolic space and use the aggregated embeddings to predict potential alignment results. Extensive experiments and ablation studies demonstrate the effectiveness of our proposed model and its components.

*Keywords:* Multi-modal knowledge graphs, Entity alignment, Hyperbolic Graph Convolutional Networks, Hyperboloid manifold

---

## 1. Introduction

Over recent years, knowledge graph (KG) has become a popular data structure for representing factual knowledge in the form of RDF triples, which

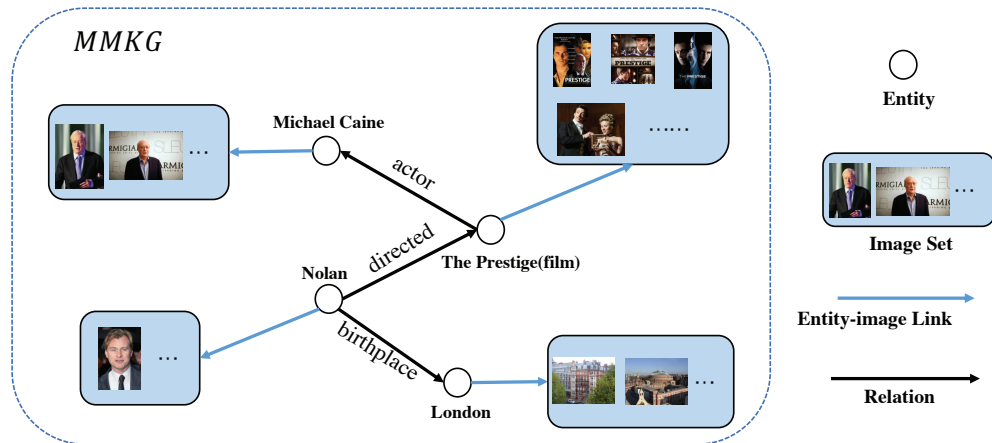


Figure 1: An example of MMKG.

can facilitate a pile of downstream applications such as question answering [9], information extraction [46], etc. Currently, we have a large number of general KGs (e.g., DBpedia [1], YAGO [35], Google’s Knowledge Vault [12]), and domain-specific KGs (e.g., Medical and Molecule KGs).

Meanwhile, there is a growing trend to incorporate multi-media information into KGs, so as to support cross-modal tasks that involve the interactions of data in multiple modalities, e.g., image and video retrieval [40], video summaries [30], visual entity disambiguation [28], and visual question answering [47], etc. To this end, several multi-modal KGs (MMKGs) [26, 41] have been constructed very recently. An example of MMKG can be found in Figure 1. In this work, without losing generality, we consider MMKG with two modalities, i.e., the KG structure information and visual information.

**Example 1.** *Figure 1 shows a partial MMKG, which consists of entities, image sets and the links between them. Specifically, the KG structure information includes the relations among entities, while the visual information comes from the image sets. For the entity *ThePrestige*, its image set may contain scenes, actors, posters, etc.*

Nevertheless, existing MMKGs usually come from limited data sources, and hence might suffer from low coverage of the domain [33]. To improve the coverage of these MMKGs, a possible approach is to integrate useful knowledge from other MMKGs. Particularly, identifying equivalent entities in different KGs is a pivotal step to consolidate the knowledge among MMKGs,

since entities are the anchors that connect these heterogeneous KGs. This process is also termed as multi-modal entity alignment (MMEA).

MMEA is a non-trivial task, as it requires the modeling and integration of multi-modal information. For the *KG structure information*, existing entity alignment (EA) approaches [17, 7, 37, 48] can be directly adopted to generate entity structural embeddings for MMEA. These methods usually utilize TransE-based or graph convolutional network(GCN)-based models [2, 21] to learn entity representations of individual KGs, which are then unified using the seed entity pairs. Nevertheless, all of these methods learn entity representations in the Euclidean space, which leads to a large distortion when embedding real-world graphs with scale-free or hierarchical structure [8, 34]. Regarding the *visual information*, the VGG16 model has been harnessed to learn the embeddings of images associated with entities and then used for alignment. However, the VGG16 model cannot sufficiently extract useful features from images, which in turn constrains the effectiveness of alignment. Last but not least, the information from these two modalities should be carefully integrated so as to improve the overall effectiveness.

To address the aforementioned issues, in this work, we propose a multi-modal entity alignment approach that operates in Hyperbolic Space (HMEA). Specifically, we extend the Euclidean representation to hyperboloid manifold and adopt the Hyperbolic Graph Convolutional Networks (HGCMs) to learn structural representations of entities. Regarding the visual information, we generate image embeddings using the densenet model, which are also projected into the Hyperbolic space using HGCMs. Finally, we merge the structure embeddings and image embeddings in the hyperbolic space to predict potential alignments.

In summary, the major contributions of our approach can be summarized as follows:

- We propose a novel MMEA approach, HMEA, which models and integrates multi-modal information in the hyperbolic space.
- We adopt the Hyperbolic Graph Convolutional Networks (HGCMs) to learn structural representations of entities and demonstrate the advantage of Hyperbolic space for knowledge graph representations.
- We utilize a more advanced image embedding model to learn better visual representations for alignment.

- We validate the effectiveness of our proposed model via comprehensive experimental evaluations.

*Organization.* Section 2 overviews related work, and the preliminaries are introduced in Section 3. Section 4 describes our proposed approach. Section 5 presents experimental results, followed by conclusion in Section 6.

## 2. Related Work

In this section, we introduce some efforts that are relevant to this work.

### 2.1. Multi-modal Knowledge Graph

Most of the knowledge graph construction works focus on organizing and discovering textual knowledge in a structured representation, while paying little attention to other types of resources on the Web [41]. Nevertheless, real-life applications involve cross-modal data, such as image and video retrieval, video summaries, visual question answering, visual commonsense reasoning, etc. To this end, Multi-modal Knowledge Graphs(MMKGs) are put forward, which contain various information (i.e. image, text, KG) and cross-modal relations. However, there are several challenges in building MMKGs. Extracting massive data of multiple modalities from search engines to build them is a time-consuming and labor-intensive project. In addition, MMKGs usually suffer from low coverage of the domain and are incomplete. Integrating multi-modal knowledge from other MMKGs is an efficient approach to improve its completeness. Currently, there are few studies about merging different MMKGs. Liu et al. [26] built two pairs of MMKGs, and extracted relational, latent, numerical and visual features for predicting the *SameAs* link between entities. And some approaches of multi-modal knowledge representation involve visual features from entity images for knowledge representation learning, IKRL [45] integrates image representations into an aggregated image-based representation via an attention-based method.

### 2.2. Entity Alignment

Over recent years, there are many works dedicated to the task of entity alignment [20], which could be used to model the structural information of MMKGs. Entity alignment is the task of finding equivalent entities in two KGs that refer to the same real-world object, which plays a pivotal step in automatically consolidating knowledge among KGs [7, 17, 49]. In general,

current EA approaches mainly tackle the problem by assuming that equivalent entities in different KGs possess similar neighboring structure, and employing representation learning methods to embed entities as data points in a low-dimensional feature space. The distance between data points is used to evaluate the similarity of corresponding entities.

There are mainly two types of embedding learning models. TransE-based models [3] suggest that the embedding of the tail entity  $t$  should be close to the embedding of the head entity  $h$  plus the embedding of the relationship  $r$ . Meanwhile, Graph neural networks (GNN) have received increased attention due to their attractive properties for learning from graph-structured data [4]. Originally proposed in [15], as a method for learning node representations on graphs using neural networks, this idea was extended to convolutional neural networks using spectral methods [10]. Graph convolutional network(GCN) can directly operate on graph-structured data and generate node-level embeddings by encoding the information about node neighborhoods. GCN-align [42] uses GCN to learn the structure and attribute information, then combines them with a balanced weight. Noticing that GCN neglects the relations in KGs, RDGCN [43] adopts the dual-primal graph convolutional neural network (DPGCNN) [27] as a remedy. MuGNN [5], on the other hand, utilizes an attention-based GNN model to assign different weights to different neighboring nodes. KECCG [25] combines the graph attention network (GAT) [39] and TransE to capture both the inner-graph structure and the inter-graph alignment information.

### *2.3. Representation Learning in Hyperbolic Space*

Essentially, most of the existing GCNs models are designed for the graphs in Euclidean spaces. [6] However, some works have discovered that graph data exhibits a non-Euclidean latent anatomy [29], and embedding real-world graphs with scale-free or hierarchical structure leads to a large distortion [8, 34]. Additionally, several recent researches in network science also show that hyperbolic geometry in particular is well-suited for modeling complex networks, as the hyperbolic space may reflect some properties of graph naturally [23]. One key property of hyperbolic spaces is that they expand faster than Euclidean spaces, because Euclidean spaces expand polynomially while hyperbolic spaces expand exponentially. Due to the natural advantage of hyperbolic space for graph structure data representation, representation learning in hyperbolic spaces has received increasing attention,

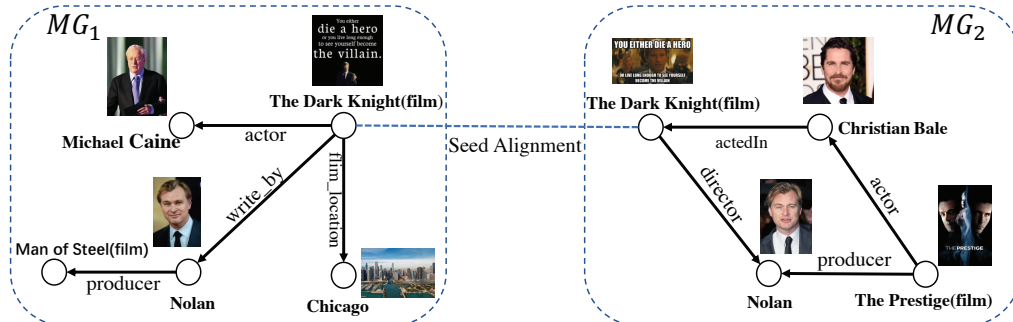


Figure 2: An example of MMEA. Seed entity pairs are connected by dashed lines. For clarity, we only choose an image to represent the set of images of an entity.

especially on learning the hierarchical representation of a graph [31]. Furthermore, Nickel et al. [32] showed that the Lorentz model of hyperbolic geometry has attractive properties for stochastic optimization and leads to substantially improved embeddings, especially in low dimensions. Besides, some researches began to extend deep learning methods to hyperbolic space and showed state-of-the-art performance on link prediction and node classification tasks [14, 16, 38].

### 3. Preliminaries

In this section, we first formally define the task of MMEA, and then we briefly review the GCN model. Finally, we introduce the basic concepts of hyperbolic geometry, which serve as building blocks for our proposed model.

#### 3.1. Task Formulation

MMEA aims to align entities in two MMKGs. A MMKG usually contains information in multiple modalities. In this work, without loss of generality, we focus on the KG structure information and visual information. Formally, we represent a MMKGs as  $MG = (E, R, T, I)$ , where  $E$ ,  $R$ ,  $T$ , and  $I$  denote the sets of entities, relations, triples and images, respectively. A relational triple  $t \in T$  can be represented as  $(e_1, r, e_2)$ , where  $e_1, e_2 \in E$  and  $r \in R$ . An entity  $e$  is associated with multiple images  $I_e = \{i_e^0, i_e^1, \dots, i_e^n\}$ .

Given two MMKGs,  $MG_1 = (E_1, R_1, T_1, I_1)$ ,  $MG_2 = (E_2, R_2, T_2, I_2)$ , and seed entity pairs (pre-aligned entity pairs for training)  $S = \{(e_s^1, e_s^2) | e_s^1 \leftrightarrow e_s^2, e_s^1 \in E_1, e_s^2 \in E_2\}$ , where  $\leftrightarrow$  represents equivalence, the task of MMEA can

be defined as discovering more aligned entity pairs  $\{(e^1, e^2) | e^1 \in E_1, e^2 \in E_2\}$ . We use Example 2 to further illustrate this task.

**Example 2.** *Figure 2 shows two partial MMKGs. The equivalence between **The Dark Knight** in  $MG_1$  and **The Dark Knight** in  $MG_2$  is known in advance. EA aims to detect potential equivalent entity pairs, e.g., **Nolan** in  $MG_1$  and **Nolan** in  $MG_2$ , using the known alignments.*

### 3.2. Graph Convolutional Neural Networks

GCNs [18, 22] are a type of neural network that directly operates on graph data. A GCN model consists of multiple stacked GCN layers. The inputs to the  $l$ -th layer of the GCN model are feature vectors of nodes and the structure of the graph.  $\mathbf{H}^{(l)} \in R^{n \times d^l}$  is a vertex feature representation, where  $n$  is the number of vertices and  $d^l$  is the dimensionality of feature matrix.  $\hat{\mathbf{A}} = \mathbf{D}^{-\frac{1}{2}}(\mathbf{A} + \mathbf{I})\mathbf{D}^{-\frac{1}{2}}$  represents the symmetric normalized adjacency matrix. The identity matrix  $\mathbf{I}$  is added to the adjacency matrix  $\mathbf{A}$  to obtain self-loops for each node, and the degree matrix  $\mathbf{D} = \sum_j (\mathbf{A}_{ij} + \mathbf{I}_{ij})$ . The output of the  $l$ -th layer is a new feature matrix  $\mathbf{H}^{(l+1)}$  by the following convolutional computation:

$$\mathbf{H}^{(l+1)} = \sigma(\hat{\mathbf{A}}\mathbf{H}^{(l)}\mathbf{W}^{(l)}). \quad (1)$$

### 3.3. Hyperboloid Manifold

We briefly review the key notions from the hyperbolic geometry; a more in-depth description is available in [13]. Hyperbolic geometry is a non-Euclidean geometry with constant negative curvature that measures how a geometric object deviates from a flat plane. In this work, we use the  $d$ -dimensional Poincare ball model with negative curvature  $-c$  ( $c > 0$ ):  $P^{(d,c)} = \{\mathbf{x} \in R^d : \|\mathbf{x}\|^2 < \frac{1}{c}\}$ , where  $\|\cdot\|$  is the  $L_2$  norm. For each point  $x \in P^{(d,c)}$ , the tangent space  $T_x^c$  is a  $d$ -dimensional vector space at point  $x$ , which contains all possible directions of paths in  $P^{(d,c)}$  leaving from  $x$ . Then, we introduce some basic operations in the hyperbolic space, which are essential in our proposed model.

**Exponential and logarithmic maps.** Specifically, let  $\mathbf{v}$  be the feature vector in the tangent space  $T_{\mathbf{o}}^c$ ;  $\mathbf{o}$  is a point in the hyperbolic space  $P^{(d,c)}$ , which is also used as a reference point. Let  $\mathbf{o}$  be the origin,  $\mathbf{o} = 0$ . The tangent space  $T_{\mathbf{o}}^c$  can be mapped to  $P^{(d,c)}$  via the exponential map:

$$\text{exp}_{\mathbf{o}}^c(\mathbf{v}) = \tanh(\sqrt{c}\|\mathbf{v}\|) \frac{\mathbf{v}}{\sqrt{c}\|\mathbf{v}\|}. \quad (2)$$

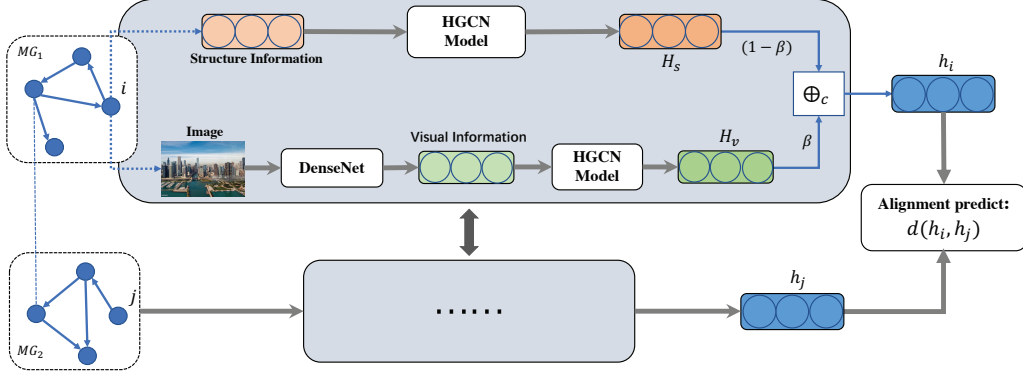


Figure 3: The framework of our proposed method.

And conversely, the logarithmic map which maps  $P^{(d,c)}$  to  $T_o^c$  is defined as:

$$\log_o^c(\mathbf{y}) = \operatorname{arctanh}(\sqrt{c}\|\mathbf{y}\|) \frac{\mathbf{y}}{\sqrt{c}\|\mathbf{y}\|}. \quad (3)$$

**Möbius addition.** Vector addition is not well-defined in the hyperbolic space and adding the vectors of two points straightly like Euclidean in the Poincare ball might result in a point outside the ball. In this case, the Möbius addition [14] provides an analogue to the Euclidean addition in the hyperbolic space. Here,  $\oplus_c$  represents the Möbius addition as:

$$\mathbf{h}_i \oplus_c \mathbf{h}_j = \frac{(1 + 2c \langle \mathbf{h}_i, \mathbf{h}_j \rangle + c \|\mathbf{h}_j\|^2) \mathbf{h}_i + (1 - c \|\mathbf{h}_i\|^2) \mathbf{h}_j}{1 + 2c \langle \mathbf{h}_i, \mathbf{h}_j \rangle + c^2 \|\mathbf{h}_i\|^2 \|\mathbf{h}_j\|^2}. \quad (4)$$

#### 4. Methodology

In this section, we present our proposed approach HMEA, which operates in the hyperbolic space. The framework is shown in Figure 3. We first adopt HGCNs to learn the structural embeddings of entities. Then, we convert the images associated with entities into visual embeddings using the densenet model, which are also projected into the hyperbolic space. Finally, we combine these embeddings in the hyperbolic space and predict the alignment results using a pre-defined hyperbolic distance. We use Example 3 to illustrate our proposed model.

**Example 3.** *Further to Example 2, by using structural information, it is easy to detect that **Nolan** in  $MG_1$  is equivalent to **Nolan** in  $MG_2$ . Nevertheless, merely using structural information is not enough, which might wrongly align **Michael Caine** in  $MG_1$  to **Christan Bale** in  $MG_2$ . In this case, the visual information would be very useful, since the images of **Michael Caine** in  $MG_1$  and **Christan Bale** in  $MG_2$  are very different. Therefore, we take into account both structural and visual information for alignment.*

In the following, we introduce the components of our proposal in detail.

#### 4.1. Structural Representation Learning

We learn the structure representation of MMKGs by Hyperbolic Graph Convolutional Neural Networks, extending convolutional computation to manifold space, which benefits from the expressiveness of both graph neural networks and hyperbolic embeddings. More specifically, we first map input Euclidean features into hyperboloid manifold. Then, through *feature transformation*, *message passing* and *non-linear activation* in the hyperbolic space, we can get the hyperbolic structural representations.

**Mapping input features to hyperboloid manifold.** In general, the input node features are produced by pre-trained Euclidean neural networks, and hence, they exist in the Euclidean space. To make the features available in the hyperbolic space, we first derive a mapping from Euclidean features to hyperbolic space.

Here, we assume that the input Euclidean features  $\mathbf{x}^E \in T_{\mathbf{o}}H_c$ , where  $T_{\mathbf{o}}H_c$  represent the tangent space referring to  $\mathbf{o}$ , and  $\mathbf{o} \in H_c$  denotes the north pole (origin) in hyperbolic space. We obtain the hyperbolic feature matrix  $\mathbf{x}^H$  via:  $\mathbf{x}^H = \exp_{\mathbf{o}}^c(\mathbf{x}^E)$ , where  $\exp_{\mathbf{o}}^c(\cdot)$  is defined in Equation 2.

**Feature transformation and propagation.** Similar to GCN, feature transformation and message passing are also the core operations in hyperbolic structural learning. The operations are well-understood in the Euclidean space, however, their counterparts in hyperboloid manifold are non-trivial. In this connection, we could execute the functions with trainable parameters in the *tangent space* of a point in the hyperboloid manifold, since the tangent space is Euclidean. To this end, we leverage the  $\exp(\cdot)$  map and  $\log(\cdot)$  map to transform between hyperboloid manifold and the tangent space, so that we can use the tangent space  $T_{\mathbf{o}}H_c^d$  to perform Euclidean operations.

We first use the logarithmic map to project hyperbolic representation  $\mathbf{x}_v^H \in R^{1 \times d}$  of node  $v$  to the tangent space  $T_{\mathbf{o}}H_c^d$ . And in  $T_{\mathbf{o}}H_c^d$ , feature transformation and propagation rule for  $v$  is calculated as:

$$\mathbf{x}_v^T = \hat{\mathbf{A}} \log_{\mathbf{o}}^c(\mathbf{x}_v^H) \mathbf{W}, \quad (5)$$

where  $\mathbf{x}_v^T \in R^{1 \times d'}$  denotes the feature representation in the tangent space and  $\hat{\mathbf{A}}$  represents the symmetric normalized adjacency matrix;  $\mathbf{W}$  is a  $d' \times d$  trainable weight matrix.

**Non-linear activation with different curvatures.** After getting the representation in the tangent space, we use a non-linear activation function  $\sigma^{\otimes c_l, c_{l+1}}$  to learn non-linear transformations. More concretely, in  $l$  layer’s tangent space  $T_{\mathbf{o}}H_{c_l}^d$ , we conduct Euclidean non-linear activation. Then we map it to the manifold of the next layer:

$$\sigma^{\otimes c_l, c_{l+1}}(\mathbf{x}_v^T) = \exp_{\mathbf{o}}^{c_{l+1}}(\sigma(\log_{\mathbf{o}}^{c_l}(\mathbf{x}_v^T))), \quad (6)$$

where  $-1/c_l, -1/c_{l+1}$  are hyperbolic curvatures at layer  $l$  and  $l + 1$ , respectively; the activation function  $\sigma$  is chosen as  $\text{ReLU}(\cdot)$ . This step is significant as it allows us to smoothly vary the curvature at each layer, which is crucial to the overall performance due to the limited machine precision and normalization.

Based on the hyperboloid feature transformation and non-linear activation, the convolutional computation in the hyperbolic space is redefined as:

$$\mathbf{H}^{l+1} = \exp_{\mathbf{o}}^{c_{l+1}}(\sigma(\hat{\mathbf{A}} \log_{\mathbf{o}}^{c_l}(\mathbf{H}^l) \mathbf{W})), \quad (7)$$

where  $\mathbf{H}^{l+1} \in R^{n \times d^{l+1}}$ ,  $\mathbf{H}^l \in R^{n \times d^l}$  are the learned node embeddings in the hyperbolic space at  $l + 1$  layer and  $l$  layer; and  $\mathbf{H}^0 = \mathbf{x}^H$ ;  $\hat{\mathbf{A}}$  represents the symmetric normalized adjacency matrix;  $\mathbf{W}$  is a  $d^l \times d^{l+1}$  trainable weight matrix.

#### 4.2. Visual Representation Learning

We adopt the `densenet` model [19] to learn image embeddings, which is pre-trained on the ImageNet dataset [11]. We remove the softmax layer in `densenet` and obtain the 1920-dimensional embeddings for all images in the MMKGs. Then, we project the embeddings into the hyperbolic space using HGCNs to improve their expressiveness.

### 4.3. Multi-modal Information Fusion

Both of the visual and structural information can contribute to the alignment results, as shown in Example 3. Therefore, we design a novel method to combine *structure information* and *visual information* of MMKGs. More specifically, we obtain the merged representation of entity  $\mathbf{e}_i$  in hyperbolic space via:

$$\mathbf{h}_i = (\beta \cdot \mathbf{H}_s^i) \oplus_c ((1 - \beta) \cdot \mathbf{H}_v^i), \quad (8)$$

where  $\mathbf{H}_s$  and  $\mathbf{H}_v$  are structure and visual embeddings learned from HGCNs model, respectively;  $\beta$  is a hyper-parameter to balance the significance of these two features; the operator  $\oplus_c$  is the Möbius addition. The combination requires the dimensions of structural and visual representations to be the same.

### 4.4. Alignment Prediction

We predict the alignment results based on the distance between entity representations from two MMKGs. The Euclidean distance and Manhattan distance are commonly used distance measures in the Euclidean space [44, 24]. Nevertheless, in the hyperbolic space, we have to utilize the hyperbolic distance between nodes as the distance measure. For entities  $e_i$  in  $MG_1$  and  $e_j$  in  $MG_2$ , the distance is defined as:

$$d_c(\mathbf{h}_i, \mathbf{h}_j) = \|(-\mathbf{h}_i) \oplus_c \mathbf{h}_j\|, \quad (9)$$

where  $\mathbf{h}_i$  and  $\mathbf{h}_j$  denote the merged embeddings of  $e_i$  and  $e_j$  in the hyperbolic space, respectively;  $\|\cdot\|$  is the  $L_1$  norm; the operator  $\oplus_c$  is the Möbius addition.

The distance is expected to be small for equivalent entities and large for non-equivalent ones. For a specific entity  $e_i$  in  $MG_1$ , our approach computes the distances between  $e_i$  and all the entities in  $MG_2$ , and returns a list of ranked entities as candidate alignments.

### 4.5. Model Training

In order to embed equivalent entities as close as possible in the vector space, we use a set of known entity alignments (seed entities)  $S$  as training data to train the model. Concretely, the model training is performed by minimizing the following margin-based ranking loss function:

$$L = \sum_{(e,v) \in S} \sum_{(e',v') \in S'_{(e,v)}} [d_c(\mathbf{h}_e, \mathbf{h}_v) + \gamma - d_c(\mathbf{h}_{e'}, \mathbf{h}_{v'})]_+, \quad (10)$$

where  $[x]_+ = \max\{0, x\}$ ;  $(e, v)$  represents a seed entity pair and  $S$  is the set of entity pairs;  $S'_{(e,v)}$  denotes the set of negative instances constructed by corrupting  $(e, v)$ , i.e., replacing  $e$  or  $v$  with a randomly chosen entity in  $MG1$  or  $MG2$ ;  $\gamma > 0$  denotes the margin hyper-parameter separating positive and negative instances. The margin-based loss function requires that the distance between the entities in positive pairs should be small, and the distance between the entities in negative pairs should be large.

## 5. Experiment

### 5.1. Dataset and Evaluation Metric

In the experiment, we use the datasets built in [26], which are extracted from FreeBase, DBpedia, and YAGO respectively. These datasets use FB15K as a starting point to create the multi-modal knowledge graphs. Then they align the entities in FB15K with entities in others knowledge graphs using the reference links, resulting in DB15K and YAGO15K. We conducted experiments on two pairs of MMKGs, namely, FB15K-DB15K and FB15K-YAGO15K.

Table 1: Statistic of the MMKGs Datasets.

Datasets	Entities	Relations	Rel.Triples	Images	SameAs
FB15K	14,951	1,345	592,213	13,444	
DB15K	14,777	279	99,028	12,841	12,846
YAGO15K	15,404	32	122,886	11,194	11,199

Since the datasets do not provide the original pictures, to obtain the relevant images for each entity, we use the URIs built in [28] and implement a web crawler that is able to parse query results from the image search engines, i.e., Google Images <sup>1</sup>, Bing Images <sup>2</sup>, and Yahoo Image Search <sup>3</sup>. Then, we assign the pictures obtained by different search engines to different MMKGs, so as to reflect the heterogeneity of different MMKGs.

Table 1 outlines the detailed information of the datasets. Each dataset contains nearly 15 thousand entities and more than 11 thousand image sets of entity. The *Images* column represents the number of entities that possess

<sup>1</sup><https://www.google.com/imghp?hl=EN>

<sup>2</sup><https://www.bing.com/image>

<sup>3</sup><https://images.search.yahoo.com/>

the image sets. These alignments are given by the *SameAs* predicates that have been previously found. In the experiments, the known equivalent entity pairs are used for model training and testing.

**Evaluation metric.** We use *Hits@k* as the evaluation measure to assess the performance of all the approaches. *Hits@k* measures the proportion of correct aligned entities ranked in the top- $k$  candidates.

### 5.2. Experiment Setting and Competing Approaches

**Experiment Setting.** In order to assess the performance under different percentages of the given alignments  $P(\%)$ , we evaluate the methods with low (20%), medium (50%) and high percentage (80%) of the given seed entity pairs. The remaining *sameAs* triples are used for test. For fairness, we keep the number of dimensions to be the same (i.e., 400) for **GCN-align** and **HMEA**. The other parameters of **GCN-align** follow [42]. For the parameters of our approach **HMEA**, we generate 6 negative samples for each positive one; the margin hyper-parameters in the loss function are  $\gamma_{\text{HMEA}-s} = 0.5$  and  $\gamma_{\text{HMEA}-v} = 1.5$ , respectively. We optimize **HMEA** with *Adam*.

**Competing approaches.** To demonstrate the superiority of our proposed model, we chose three state-of-the-art approaches as competitors:

- **GCN-align** [42] adopts GCN to encode the structural information of entities, and then combines relation and image embeddings for the entity alignment task.
- **PoE** [26] is the product of experts model. It computes the scores of facts under each modality, and learns the entity embeddings for entity alignment. **PoE** combines information from two modalities. We also compare with the variant **PoE-s**, which merely uses the structure information.
- **IKRL** [45] integrates image representations into an aggregated image-based representation via an attention-based method. It is originally proposed in the field of knowledge representation and we adopt it to tackle **MMEA**.

To further demonstrate the benefit from hyperbolic geometry, especially in learning structural features, we conduct exploratory experiments by solely using *structure information* for EA, resulting in **HMEA-s**, **GCN-align-s** and

PoE-s. In addition, to evaluate the contribution of *visual information*, we compare PoE, GCN-align and HMEA with just *visual information*, namely PoE-v, GCN-align-v and HMEA-v.

### 5.3. Results

The results are shown in Table 2. It is obvious that HMEA achieves the best performance in all cases. Especially in FB15K-YAGO15K, with 80% seed entity pairs, HMEA outperforms PoE and GCN-align by nearly 15% in terms of *Hits@1*. With 20% seed entity pairs, our approach also shows better results and the improvement of *Hits@1* is around 2% and *Hits@10* is up to 20%. According to the results of PoE, we can find that there is little enhancement from *Hits@1* to *Hits@10*, ranging from 4% to 9%. In contrast, the enhancements from *Hits@1* to *Hits@10* of HMEA are at least 20% in all situations. By the way, HMEA outperforms IKRL by a large margin.

Table 2: Alignment prediction on both datasets for different percentages of P.

FB15K-DB15K	20%		50%		80%	
	<i>Hits@1</i>	<i>Hits@10</i>	<i>Hits@1</i>	<i>Hits@10</i>	<i>Hits@1</i>	<i>Hits@10</i>
PoE	11.1	17.8	23.5	33.0	34.4	40.6
GCN-align	5.35	17.11	13.85	34.31	22.18	48.95
IKRL	1.01	2.40	2.77	5.79	5.41	11.09
HMEA	<b>12.65</b>	<b>36.86</b>	<b>26.23</b>	<b>58.08</b>	<b>41.68</b>	<b>78.55</b>
FB15K-YAGO15K	20%		50%		80%	
	<i>Hits@1</i>	<i>Hits@10</i>	<i>Hits@1</i>	<i>Hits@10</i>	<i>Hits@1</i>	<i>Hits@10</i>
PoE	8.7	13.3	18.5	24.7	28.9	34.3
GCN-align	6.76	17.99	16.47	35.85	28.75	53.05
IKRL	0.86	1.75	1.95	3.73	3.57	7.14
HMEA	<b>10.51</b>	<b>31.27</b>	<b>26.50</b>	<b>58.08</b>	<b>43.30</b>	<b>80.11</b>

As shown in Table 3, if solely using *structural information*, HMEA-s still leads to better results than other two methods. More concretely, our proposed approach outperforms GCN-align-s by nearly 5% on FB15K-DB15K and 3% on FB15K-YAGO15K in terms of *Hits@1* with 20% seed alignments. With 50% and 80% seed entity pairs, HMEA-s brings significantly better results. The improvements range from 10% to 18% regarding *Hits@1* and from 20% to 30% in terms of *Hits@10*. According to the results, it can be concluded that our approach does have advantage in capturing accurate hierarchical structure representation.

Table 3: Results of three methods with *structure information*.

FB15K-DB15K	20%		50%		80%	
	<i>Hits@1</i>	<i>Hits@10</i>	<i>Hits@1</i>	<i>Hits@10</i>	<i>Hits@1</i>	<i>Hits@10</i>
PoE-s	10.7	16.5	22.9	31.7	33.6	38.6
GCN-align-s	5.35	17.11	13.85	34.31	22.18	48.95
HMEA-s	<b>11.73</b>	<b>33.56</b>	<b>24.84</b>	<b>56.69</b>	<b>40.87</b>	<b>76.77</b>
FB15K-YAGO15K	20%		50%		80%	
	<i>Hits@1</i>	<i>Hits@10</i>	<i>Hits@1</i>	<i>Hits@10</i>	<i>Hits@1</i>	<i>Hits@10</i>
PoE-s	8.4	12.3	18.0	23.1	28.1	31.9
GCN-align-s	6.76	17.99	16.47	35.85	28.75	53.05
HMEA-s	<b>9.66</b>	<b>28.96</b>	<b>25.37</b>	<b>56.60</b>	<b>42.63</b>	<b>78.42</b>

With *visual information* (Table 4), we compare three variants: PoE-v, GCN-align-v and HMEA-v. It is obvious that GCN-align does not obtain useful visual representation for MMEA. If solely using structural information, HMEA-v still shows better results than PoE-v. More concretely, our proposed approach outperforms PoE-v slightly with 20% seed alignments, less than 1% on both datasets regarding *Hits@1*. With 80% seeds on FB15K-DB15K, HMEA-v brings significantly better results. The improvements are around 7% regarding *Hits@1* and 18% in terms of *Hits@10*. The results demonstrate the effectiveness of our proposed mode for learning visual features.

Table 4: Comparison of three methods with *visual information*.

FB15K-DB15K	20%		50%		80%	
	<i>Hits@1</i>	<i>Hits@10</i>	<i>Hits@1</i>	<i>Hits@10</i>	<i>Hits@1</i>	<i>Hits@10</i>
PoE-v	0.8	2.7	1.3	3.8	1.7	5.9
GCN-align-v	0.0	0.0	0.0	0.0	0.0	0.0
HMEA-v	<b>1.77</b>	<b>8.08</b>	<b>3.33</b>	<b>12.65</b>	<b>9.05</b>	<b>24.20</b>
FB15K-YAGO15K	20%		50%		80%	
	<i>Hits@1</i>	<i>Hits@10</i>	<i>Hits@1</i>	<i>Hits@10</i>	<i>Hits@1</i>	<i>Hits@10</i>
PoE-v	0.7	2.4	1.1	3.2	1.7	5.5
GCN-align-v	0.0	0.0	0.0	0.0	0.0	0.0
HMEA-v	<b>1.35</b>	<b>5.43</b>	<b>2.71</b>	<b>11.15</b>	<b>5.79</b>	<b>18.07</b>

#### 5.4. Ablation Experiment

MMKGs consist of information in multiple modalities. We take the structural and visual information into account in this work. In order to further validate the effectiveness of multi-modal knowledge for MMEA, we conduct the ablation experiment. By comparing HMEA and HMEA-s in Table 2 and Table 3, it can be seen that adding *visual information* in our approach does lead to slightly better results and the improvements are around 1% in terms

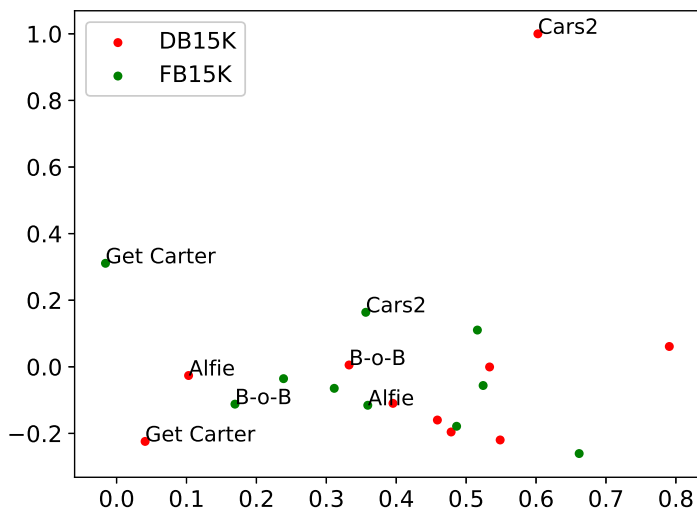
of *Hits@1*. Moreover, by comparing HMEA and HMEA-v in Table 2 and Table 4, we can also see that the structural information is of great significance. The ablation study shows that MMEA mainly relies on the *structural information*, but the *visual information* is still useful. In addition, it demonstrates that the combination of these information works much better.

### 5.5. Case Study

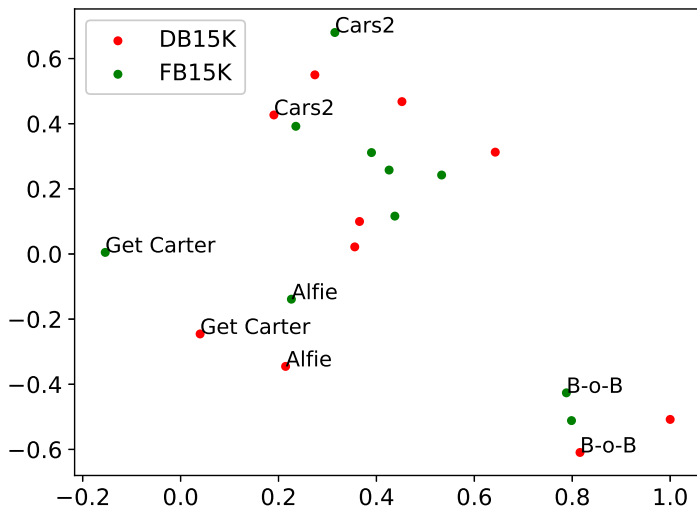
One key property of hyperbolic spaces is that they expand faster than Euclidean spaces, because Euclidean spaces expand polynomially while hyperbolic spaces expand exponentially. In other words, for the neighbor nodes of the central node, they are distributed in bigger space and the distances between them are farther, which can help distinguish similar entities.

To further demonstrate the effectiveness of the embeddings in hyperbolic space, we conduct the following case study. We choose Michael Caine as the root node. We visualize the embeddings of its 1-hop film-related entities learned from GCN-align and HMEA separately in the PCA-projected spaces in Figure 4. It can be observed that, for the entities of the same type or with similar structure information, especially for entity **Alfie** and **B-o-B**, their Euclidean embeddings (generated via GCN-align) are placed closely. While in Hyperbolic space, the distances between such entities are relatively farther away (with only a few exceptions). This validates that the hyperbolic structure representation can help distinguish similar entities. Moreover, by placing similar entities (in the same KG) distantly, the hyperbolic representation can help the alignment process (alignment across KG).

For instance, as shown in Figure 4(a), for entity **Alfie** in FB15K, the closest entity to it is entity **B-o-B** (which is incorrect). However, in Figure 4(b), for entity **Alfie**, the entity **B-o-B** is placed far away from it, and the closest entity to it is **Alfie** in DB15K. Hence, by using the hyperbolic projection, similar entities in the same KG are well distinguished and placed far away, such that alignment mistakes could be avoided.



(a) Embedding generated from GCN-align



(b) Embedding generated from HMEA

Figure 4: The embeddings of 1-hop film-related neighbor entities of **Michael Caine** generated from GCN-align and HMEA separately in the PCA-projected space. The green points represent entities in FB15K; red points represent entities in DB15K. For simplicity, we annotate part of entities. **B-o-B** is the abbreviation of **Battle of Britain**.

## 5.6. Additional Experiment

Table 5: **Details of the cross-lingual datasets**

Datasets		Entities	Relations	Attributes	Rel.triples	Attr.triples
DBP15K <sub>ZH-EN</sub>	Chinese	66,469	2,830	8,113	153,929	379,684
	English	98,125	2,137	7,173	237,674	567,755
DBP15K <sub>JA-EN</sub>	Japanese	65,744	2,043	5,882	164,373	354,619
	English	95,680	2,096	6,066	233,319	497,230
DBP15K <sub>FR-EN</sub>	French	66,858	1,379	4,547	192,191	528,665
	English	105,889	2,209	6,422	278,590	576,543

The cross-lingual EA datasets are the most widely-used datasets to assess EA approaches. We added the experiments on them to show that our proposed approach can work on such popular datasets (and the cross-lingual EA task). Note that diverse languages are not taken as multiple modalities, and the cross-lingual EA is in essence single-modal EA. We use the DBP15K datasets in the experiments, which were built by [36]. The datasets were generated from DBpedia, containing rich inter-language links between different language versions. Each dataset contains data in different languages and 15 thousand known inter-language links connecting equivalent entities in two KGs, which are used for model training and testing. Following the setting in [42], we use 30% of inter-language links for training, and 70% of them for testing. *Hits@k* is used as the evaluation measure.

Both the dimensions of structure and attribute are set to 300-dimension for GCN-align. GCN-align-s and HMEA-s represent adopting structure information; GCN-align-a and HMEA-a represent adopting attribute information; and GCN-align and HMEA combine both the structure information and attribute information.

As shown in Table 6, in all datasets, HMEA-s outperforms GCN-align-s and the improvements are around 7% in terms of *Hits@1* and more than 10% in terms of *Hits@10*. It demonstrates that HMEA benefits from hyperbolic geometry and is able to capture better structural features. In addition, with the combination of structure information and attribute information, our proposed approach outperforms GCN-align by around 10% regarding *Hits@1*. As for the attribute information, HMEA-a also gets significantly better results than GCN-align-a, which increases by around 15% on *Hits@1* in all datasets.

Table 6: Result in Cross-lingual datasets.

DBP15K <sub>ZH-EN</sub>	ZH-EN		EN-ZH	
	<i>Hits@1</i>	<i>Hits@10</i>	<i>Hits@1</i>	<i>Hits@10</i>
GCN-align-s	39.42	71.34	33.60	65.23
HMEA-s	<b>46.23</b>	<b>82.36</b>	<b>44.53</b>	<b>81.95</b>
GCN-align-a	13.44	40.94	12.54	38.78
HMEA-a	<b>33.99</b>	<b>71.15</b>	<b>32.80</b>	<b>69.79</b>
GCN-align	43.08	75.92	36.25	69.17
HMEA	<b>54.04</b>	<b>87.88</b>	<b>51.88</b>	<b>86.57</b>
DBP15K <sub>JA-EN</sub>	JA-EN		EN-JA	
	<i>Hits@1</i>	<i>Hits@10</i>	<i>Hits@1</i>	<i>Hits@10</i>
GCN-align-s	39.95	72.72	36.09	67.43
HMEA-s	<b>47.63</b>	<b>83.96</b>	<b>47.24</b>	<b>83.96</b>
GCN-align-a	9.27	31.85	8.78	31.89
HMEA-a	<b>28.36</b>	<b>63.99</b>	<b>27.73</b>	<b>63.97</b>
GCN-align	42.51	75.74	38.31	70.49
HMEA	<b>53.06</b>	<b>87.47</b>	<b>52.65</b>	<b>87.41</b>
DBP15K <sub>FR-EN</sub>	FR-EN		EN-FR	
	<i>Hits@1</i>	<i>Hits@10</i>	<i>Hits@1</i>	<i>Hits@10</i>
GCN-align-s	38.38	74.45	37.37	71.65
HMEA-s	<b>44.27</b>	<b>83.15</b>	<b>43.81</b>	<b>83.14</b>
GCN-align-a	2.65	13.50	3.02	14.51
HMEA-a	<b>12.40</b>	<b>48.70</b>	<b>15.44</b>	<b>52.12</b>
GCN-align	39.48	76.05	38.44	73.33
HMEA	<b>48.40</b>	<b>86.49</b>	<b>48.15</b>	<b>86.18</b>

## 6. Conclusion

In this paper, we propose HMEA, a novel multi-modal EA approach which effectively integrates multi-modal information for EA in MMKGs. It extends the Euclidean representation to hyperboloid manifold and adopts HGCNs to learn structural representations of entities. A more advanced model densenet is leveraged to learn better visual representations. The structural and visual embeddings are further aggregated in the hyperbolic space to predict potential alignments. We validate the effectiveness of our proposed model via comprehensive experimental evaluations. Additional experiments also confirm that HGCNs obtains better structural features of knowledge graphs in the hyperbolic space.

## References

- [1] S. Auer, C. Bizer, G. Kobilarov, J. Lehmann, R. Cyganiak, and Z. Ives. Dbpedia: A nucleus for a web of open data. In *The semantic web*, pages 722–735. Springer, 2007.
- [2] A. Bordes, N. Usunier, A. García-Durán, J. Weston, and O. Yakhnenko. Translating embeddings for modeling multi-relational data. In *NIPS*, pages 2787–2795, 2013.
- [3] A. Bordes, N. Usunier, A. Garcia-Duran, J. Weston, and O. Yakhnenko. Translating embeddings for modeling multi-relational data. In *Advances in neural information processing systems*, pages 2787–2795, 2013.
- [4] M. M. Bronstein, J. Bruna, Y. LeCun, A. Szlam, and P. Vandergheynst. Geometric deep learning: going beyond euclidean data. *IEEE Signal Processing Magazine*, 34(4):18–42, 2017.
- [5] Y. Cao, Z. Liu, C. Li, J. Li, and T.-S. Chua. Multi-channel graph neural network for entity alignment. *arXiv preprint arXiv:1908.09898*, 2019.
- [6] S. Cavallari, E. Cambria, H. Cai, K. C.-C. Chang, and V. W. Zheng. Embedding both finite and infinite communities on graphs [application notes]. *IEEE Computational Intelligence Magazine*, 14(3):39–50, 2019.
- [7] M. Chen, Y. Tian, M. Yang, and C. Zaniolo. Multilingual knowledge graph embeddings for cross-lingual knowledge alignment. *arXiv preprint arXiv:1611.03954*, 2016.
- [8] W. Chen, W. Fang, G. Hu, and M. W. Mahoney. On the hyperbolicity of small-world and treelike random graphs. *Internet Mathematics*, 9(4):434–491, 2013.
- [9] W. Cui, Y. Xiao, H. Wang, Y. Song, S.-w. Hwang, and W. Wang. Kbqa: learning question answering over qa corpora and knowledge bases. *arXiv preprint arXiv:1903.02419*, 2019.
- [10] M. Defferrard, X. Bresson, and P. Vandergheynst. Convolutional neural networks on graphs with fast localized spectral filtering. In *Advances in neural information processing systems*, pages 3844–3852, 2016.
- [11] J. Deng, W. Dong, R. Socher, L. Li, K. Li, and F. Li. Imagenet: A large-scale hierarchical image database. In *CVPR*, pages 248–255. IEEE Computer Society, 2009.

- [12] X. Dong, E. Gabrilovich, G. Heitz, W. Horn, N. Lao, K. Murphy, T. Strohmann, S. Sun, and W. Zhang. Knowledge vault: A web-scale approach to probabilistic knowledge fusion. In *Proceedings of the 20th ACM SIGKDD international conference on Knowledge discovery and data mining*, pages 601–610, 2014.
- [13] L. P. Eisenhart. *Introduction to differential geometry*. Princeton University Press, 2015.
- [14] O.-E. Ganea, G. Bécigneul, and T. Hofmann. Hyperbolic entailment cones for learning hierarchical embeddings. *arXiv preprint arXiv:1804.01882*, 2018.
- [15] M. Gori, G. Monfardini, and F. Scarselli. A new model for learning in graph domains. In *Proceedings. 2005 IEEE International Joint Conference on Neural Networks, 2005.*, volume 2, pages 729–734. IEEE, 2005.
- [16] C. Gulcehre, M. Denil, M. Malinowski, A. Razavi, R. Pascanu, K. M. Hermann, P. Battaglia, V. Bapst, D. Raposo, A. Santoro, et al. Hyperbolic attention networks. *arXiv preprint arXiv:1805.09786*, 2018.
- [17] Y. Hao, Y. Zhang, S. He, K. Liu, and J. Zhao. A joint embedding method for entity alignment of knowledge bases. In *China Conference on Knowledge Graph and Semantic Computing*, pages 3–14. Springer, 2016.
- [18] M. Henaff, J. Bruna, and Y. LeCun. Deep convolutional networks on graph-structured data. *arXiv preprint arXiv:1506.05163*, 2015.
- [19] G. Huang, Z. Liu, L. Van Der Maaten, and K. Q. Weinberger. Densely connected convolutional networks. In *Proceedings of the IEEE conference on computer vision and pattern recognition*, pages 4700–4708, 2017.
- [20] S. Ji, S. Pan, E. Cambria, P. Marttinen, and P. S. Yu. A survey on knowledge graphs: Representation, acquisition and applications. *arXiv preprint arXiv:2002.00388*, 2020.
- [21] T. N. Kipf and M. Welling. Semi-supervised classification with graph convolutional networks. *CoRR*, abs/1609.02907, 2016.
- [22] T. N. Kipf and M. Welling. Semi-supervised classification with graph convolutional networks. *arXiv preprint arXiv:1609.02907*, 2016.
- [23] D. Krioukov, F. Papadopoulos, M. Kitsak, A. Vahdat, and M. Boguná. Hyperbolic geometry of complex networks. *Physical Review E*, 82(3):036106, 2010.

- [24] C. Li, Y. Cao, L. Hou, J. Shi, J. Li, and T. Chua. Semi-supervised entity alignment via joint knowledge embedding model and cross-graph model. In *EMNLP*, pages 2723–2732. Association for Computational Linguistics, 2019.
- [25] C. Li, Y. Cao, L. Hou, J. Shi, J. Li, and T.-S. Chua. Semi-supervised entity alignment via joint knowledge embedding model and cross-graph model. In *Proceedings of the 2019 Conference on Empirical Methods in Natural Language Processing and the 9th International Joint Conference on Natural Language Processing (EMNLP-IJCNLP)*, pages 2723–2732, 2019.
- [26] Y. Liu, H. Li, A. Garcia-Duran, M. Niepert, D. Onoro-Rubio, and D. S. Rosenblum. Mmkg: multi-modal knowledge graphs. In *European Semantic Web Conference*, pages 459–474. Springer, 2019.
- [27] F. Monti, O. Shchur, A. Bojchevski, O. Litany, S. Günnemann, and M. M. Bronstein. Dual-primal graph convolutional networks. *arXiv preprint arXiv:1806.00770*, 2018.
- [28] S. Moon, L. Neves, and V. Carvalho. Multimodal named entity disambiguation for noisy social media posts. In *Proceedings of the 56th Annual Meeting of the Association for Computational Linguistics (Volume 1: Long Papers)*, pages 2000–2008, 2018.
- [29] A. Muscoloni, J. M. Thomas, S. Ciucci, G. Bianconi, and C. V. Cannistraci. Machine learning meets complex networks via coalescent embedding in the hyperbolic space. *Nature communications*, 8(1):1–19, 2017.
- [30] D. A. Newman and B. G. Schunck. Generating video summaries for a video using video summary templates, Oct. 17 2017. US Patent 9,792,502.
- [31] M. Nickel and D. Kiela. Poincaré embeddings for learning hierarchical representations. In *Advances in neural information processing systems*, pages 6338–6347, 2017.
- [32] M. Nickel and D. Kiela. Learning continuous hierarchies in the lorentz model of hyperbolic geometry. *arXiv: Artificial Intelligence*, 2018.
- [33] H. Paulheim. Knowledge graph refinement: A survey of approaches and evaluation methods. *Semantic web*, 8(3):489–508, 2017.
- [34] E. Ravasz and A.-L. Barabási. Hierarchical organization in complex networks. *Physical review E*, 67(2):026112, 2003.

- [35] F. M. Suchanek, G. Kasneci, and G. Weikum. Yago: a core of semantic knowledge. In *Proceedings of the 16th international conference on World Wide Web*, pages 697–706, 2007.
- [36] Z. Sun, W. Hu, and C. Li. Cross-lingual entity alignment via joint attribute-preserving embedding. In *International Semantic Web Conference*, pages 628–644. Springer, 2017.
- [37] Z. Sun, W. Hu, Q. Zhang, and Y. Qu. Bootstrapping entity alignment with knowledge graph embedding. In *IJCAI*, pages 4396–4402, 2018.
- [38] H.-N. Tran and E. Cambria. A survey of graph processing on graphics processing units. *The Journal of Supercomputing*, 74(5):2086–2115, 2018.
- [39] A. Vaswani, N. Shazeer, N. Parmar, J. Uszkoreit, L. Jones, A. N. Gomez, L. Kaiser, and I. Polosukhin. Attention is all you need. In *Advances in neural information processing systems*, pages 5998–6008, 2017.
- [40] R. C. Veltkamp, H. Burkhardt, and H.-P. Kriegel. *State-of-the-art in content-based image and video retrieval*, volume 22. Springer Science & Business Media, 2013.
- [41] M. Wang, G. Qi, H. Wang, and Q. Zheng. Richpedia: A comprehensive multi-modal knowledge graph. In *Joint International Semantic Technology Conference*, pages 130–145. Springer, 2019.
- [42] Z. Wang, Q. Lv, X. Lan, and Y. Zhang. Cross-lingual knowledge graph alignment via graph convolutional networks. In *Proceedings of the 2018 Conference on Empirical Methods in Natural Language Processing*, pages 349–357, 2018.
- [43] Y. Wu, X. Liu, Y. Feng, Z. Wang, R. Yan, and D. Zhao. Relation-aware entity alignment for heterogeneous knowledge graphs. *arXiv preprint arXiv:1908.08210*, 2019.
- [44] Y. Wu, X. Liu, Y. Feng, Z. Wang, and D. Zhao. Neighborhood matching network for entity alignment. In *ACL*, pages 6477–6487. Association for Computational Linguistics, 2020.
- [45] R. Xie, Z. Liu, H. Luan, and M. Sun. Image-embodied knowledge representation learning. pages 3140–3146, 2017.
- [46] X. Yao and B. Van Durme. Information extraction over structured data: Question answering with freebase. In *Proceedings of the 52nd Annual Meeting*

*of the Association for Computational Linguistics (Volume 1: Long Papers)*, pages 956–966, 2014.

- [47] K. Yi, J. Wu, C. Gan, A. Torralba, P. Kohli, and J. Tenenbaum. Neural-symbolic vqa: Disentangling reasoning from vision and language understanding. In *Advances in neural information processing systems*, pages 1031–1042, 2018.
- [48] W. Zeng, X. Zhao, J. Tang, and X. Lin. Collective entity alignment via adaptive features. In *ICDE*, pages 1870–1873. IEEE, 2020.
- [49] W. Zeng, X. Zhao, W. Wang, J. Tang, and Z. Tan. Degree-aware alignment for entities in tail. In *SIGIR*, pages 811–820. ACM, 2020.